

Underwater Scan Matching using a Mechanical Scanned Imaging Sonar^{*}

Antoni Burguera^{*} Yolanda González, Gabriel Oliver

^{*} *Dept. Matemàtiques i Informàtica. Universitat de les Illes Balears.
Ctra. Valldemossa Km. 7,5. 07122 Palma de Mallorca (SPAIN)
e-mail: {antoni.burguera, y.gonzalez, goliver}@uib.es.*

Abstract: Underwater environments are extremely challenging to perform localization. *Autonomous Underwater Vehicles* (AUV) are usually endowed with acoustic devices such as a *Mechanically Scanned Imaging Sonar* (MSIS). This sensor scans the environment by emitting ultrasonic pulses and it provides echo intensity profiles of the scanned area. Our goal is to provide self-localization capabilities to an AUV endowed with a MSIS. To this end, this paper proposes a scan matching strategy to estimate the robot motion. This strategy extracts range information from the sensor data, deals with the large scan times and performs a probabilistic data association. The proposal is tested with real data obtained during a trip in a marina environment, and the results show the benefits of our proposal by comparing it to other well known approaches.

Keywords: Underwater robot, localization, sonar, scan matching.

1. INTRODUCTION

First attempts to perform mobile robot localization by matching successive range scans were inspired by the computer vision community. A standard approach to image registration is the *Iterative Closest Point* (ICP) (Besl and McKay (1992)). The ICP concepts were introduced in the mobile robot localization context by Lu and Milios (1997). Due to the great success of this approach, many other scan matching algorithms rely on the same basic structure, defining the *ICP-based* family of algorithms. Examples of this family are the *Iterative Dual Correspondence* (IDC), also proposed by Lu and Milios, the *probabilistic Iterative Correspondence* (pIC) by Montesano et al. (2005) or the *the Point to Line ICP* (PLICP) presented by Censi (2008).

In general, scan matching algorithms require dense sets of accurate range readings to obtain reliable motion estimates. That is why laser sensors are often used in the context of terrestrial scan matching. However, underwater scenarios pose important limitations to light based sensors such as laser range finders. In consequence, *Autonomous Underwater Vehicles* (AUV) are usually endowed with acoustic sensors. One of these sensors is the *Mechanically Scanned Imaging Sonar* (MSIS), which scans the environment by emitting ultrasonic pulses providing echo intensity profiles of the scanned area.

When used to perform scan matching, a MSIS has two important problems. Firstly, this sensor does not provide range measurements but echo intensity profiles. Accordingly, the sensor information has to be processed before being used in the scan matching context. A simple yet effective method to perform such process has been described

by Ribas et al. (2008). Secondly, the scan time of a MSIS is not negligible. For example, in our particular configuration, the sensor needs more than 13 seconds to gather a 360° scan. Accordingly, it can not be assumed that the robot remains static while the scan is being obtained. Some considerations regarding this issue using terrestrial Polaroid sensors are provided in Burguera et al. (2008). Moreover, a recent study by Hernández et al. (2009) shows the feasibility of underwater scan matching using a MSIS.

Our goal is to provide self-localization capabilities to an AUV. To this end, this paper proposes a framework to perform scan matching in underwater environments using a MSIS. This framework includes processes to deal with the aforementioned problems of MSIS sensing. Also, a probabilistic scan matching method previously tested on terrestrial sonars, the *sonar probabilistic Iterative Correspondence* (spIC) introduced by Burguera et al. (2008), is used to perform the matching. Because of this, the framework introduced in this paper will be referred to as the *underwater spIC* (uspIC).

Section 2 overviews the underwater sonar scan matching problem. The processes to obtain range measurements from the echo intensity profiles and to deal with the large scan times are presented in sections 3 and 4 respectively. The probabilistic approach to perform scan matching is stated in section 5. Section 6 describes the processes to compute the corrected robot pose according to the scan matching estimate. Finally, sections 7 and 8 show the experimental results and conclude the paper.

2. PROBLEM STATEMENT AND NOTATION

Scan matching algorithms require two consecutively gathered sets of range measurements called *scans*. Let S_{ref} be a set of measurements gathered at frame A , which is called the *reference scan*. Let S_{cur} be a set of measurements gath-

^{*} This work is partially supported by DPI 2008-06548-C03-02, FEDER funding and FP7-TRIDENT Project SCP8-GA-2010-248497

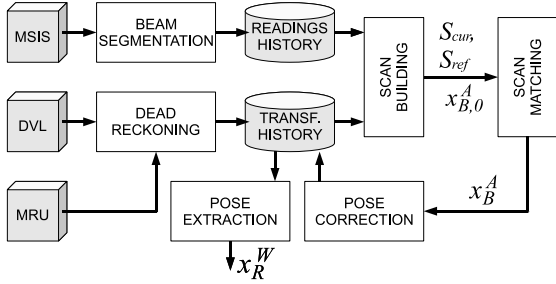


Fig. 1. Overview of the uspIC. The notation is explained throughout the paper.

ered at frame B , which is called the *current scan*. The aim of scan matching is to compute the relative displacement and rotation x_B^A of B with respect to A so that the overlap between S_{ref} and S_{cur} is maximized.

The measurements in S_{ref} and S_{cur} can be represented in different ways, depending on the specific scan matching implementation. The proposal of this paper is to represent the measurements in both scans as normal distributions, similarly to spIC. The details regarding this issue are provided in section 4. Also, in this paper the scan matching estimate is represented by a multivariate normal distribution $x_B^A = N(\hat{x}_B^A, P_B^A)$.

2.1 Scan Matching with a MSIS

The experiments conducted in this paper have been performed using the sensor data gathered by the *Ictineu AUV*. This AUV was designed and developed at the University of Girona (see Ribas et al. (2008) for more details). Among other sensors, the AUV is endowed with a *Doppler Velocity Log* (DVL) which measures the velocities of the unit with respect to bottom and water, a *Motion Reference Unit* (MRU) that provides absolute attitude data by means of compass and inclinometers, and a MSIS.

The MSIS obtains 360° scans of the environment by rotating a sonar beam through 200 angular steps in about 13.8 seconds. At each angular position, a set of 500 values, named *bins*, is obtained representing a 50 m long echo intensity profile with a resolution of 10cm. Each of these sets of 500 bins will be referred to as *beam*. By accumulating this information, an *acoustic image* of the environment can be obtained.

As stated previously, different problems arise when using a MSIS to perform scan matching. In order to solve them several processes are necessary. Our proposal is summarized in Figure 1. First, range information is extracted from each MSIS measurement by means of the *beam segmentation*. Also, DVL and MRU readings are fused by means of an *Extended Kalman Filter* (EKF) to obtain *dead reckoning* estimates, as described by Ribas et al. (2008). Both the obtained range information and the dead reckoning estimates are stored in two buffers, called *readings history* and *transformations history* respectively. When the MSIS has obtained a 360° view of the environment, the information in these buffers is used by the *scan building* to compensate the robot motion and build a scan. When two consecutive scans have been built in this way, the *scan matching* is executed. One specific scan matching method is proposed in this paper, though other algorithms can be

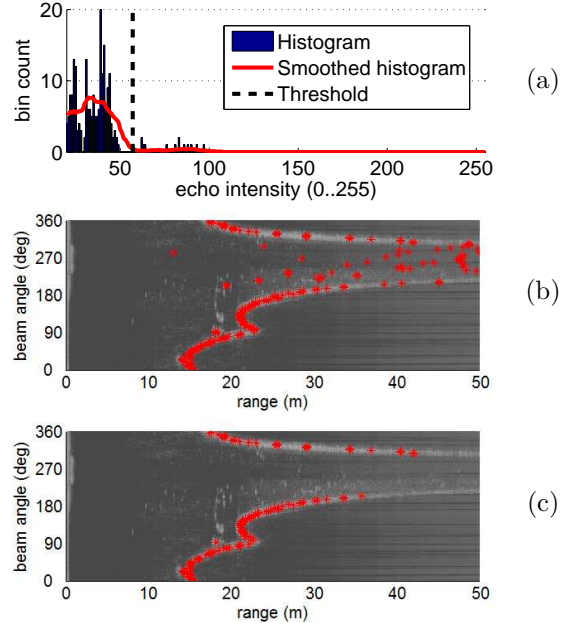


Fig. 2. (a) An example of the threshold selection process. (b) Beam segmentation example in a range vs. angle representation. The grayscale image represents the MSIS beams. The red dots depict the obtained range information selecting the maximum intensity bin. (c) The approach presented in this paper.

easily included in the uspIC framework. Finally, the *pose correction* and the *pose extraction* processes are in charge of improving the transformations history according to the matching estimate and to continuously provide robot pose information. The rest of the paper is devoted to describe the abovementioned processes.

3. BEAM SEGMENTATION

Our goal is to obtain range scans instead of the beams as they are provided by the MSIS. Accordingly, the beam segmentation is in charge of computing the distance from the sensor to the largest obstacle in the beam. Although in some cases, this distance corresponds to the bin with the largest intensity value, in some other, very frequent, cases it does not as it will be shown later. To deal with these situations, the following procedure is proposed. When the MSIS provides a new beam, the beam segmentation process obtains the corresponding range measurement by means of the following three steps:

Thresholding : An echo intensity threshold is dynamically selected as follows. Firstly, the histogram of echo intensities corresponding to the beam under analysis is computed and smoothed. Afterwards, the threshold is located at the largest echo intensity value that locally minimizes the smoothed histogram. In this way, the threshold separates two clearly defined areas in the echo intensity space. Finally, those bins whose intensity is below the threshold are discarded. Figure 2-a exemplifies the thresholding step.

Erosion : The remaining bins are eroded. That means that those bins that, after the thresholding, do not have another bin in their immediate neighborhood, are removed. The purpose of this step is to remove spurious bins.

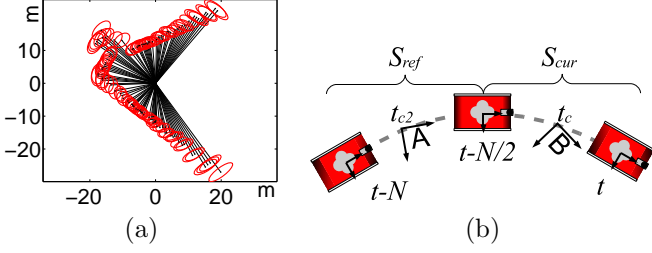


Fig. 3. (a) 95% confidence ellipses corresponding to one MSIS scan. (b) The scan building coordinate frames.

Selection : At this point, it is usual that a single cluster of bins remains. The bin with the largest echo intensity value is selected, and the distance corresponding to this bin represents the range value for the beam under analysis. Let the point corresponding to this range be named the *range reading*.

The results of selecting the maximum intensity bin and those of applying the method proposed in this paper are exemplified in Figures 2-b and 2-c respectively. It is clear that our approach is able to obtain a much more accurate range scan than a simple maximum intensity selection.

4. SCAN BUILDING

The MSIS data cannot be treated as a synchronous snapshot of the world. Instead, the sonar data is actually acquired whilst the AUV is moving. Thus, the robot motions during the sonar data acquisition have to be taken into account in order to correct the induced distortion. The *scan building* epitomizes this idea.

4.1 Modeling the Range Readings

The range readings provided by the beam segmentation constitute the range information used to build the scans. Our proposal is to model each measurement in a scan by a normal distribution. In that way, the scans not only hold information about the place where an obstacle has been detected but also about the uncertainty in this detection.

Let $r_t = N(\hat{r}_t, \sigma_t^2)$ denote a measurement obtained at time t in form of *random Gaussian variable* (RGV). Let this measurement be represented with respect to a coordinate frame centered on the MSIS and having the x axis aligned with the beam acoustic axis at time t . In this case, the mean vector has the form $\hat{r}_t = [\rho_t, 0]^T$, where ρ_t denotes the range reading provided by the beam segmentation at time t . The covariance matrix σ_t^2 is as follows:

$$\sigma_t^2 = \begin{bmatrix} \sigma_{xx}^2 & 0 \\ 0 & \sigma_{yy}^2 \end{bmatrix}, \quad (1)$$

where σ_{xx} models the range uncertainty and $\sigma_{yy} = \frac{\rho_t}{2} \tan(\frac{\alpha}{2})$ models the angular uncertainty of α degrees. The range uncertainty σ_{xx} has to be obtained experimentally, as it depends on factors such as the sensor and beam segmentation characteristics. The angular uncertainty α is tightly related to the beam's opening, and can be obtained from the MSIS specification. Figure 3-a shows an example of the readings in one MSIS scan modeled as normal distributions by showing their 95% confidence ellipses.

Let z_t represent the measurement r_t with respect to the robot coordinate frame. It is straightforward to obtain z_t

from r_t and the MSIS beam angle at time t . For the sake of simplicity, henceforth the z_t will be referred to as the sonar readings.

4.2 The scan building process

The sonar readings have to be stored in the so called *readings history* so that they can be easily accessed by the scan building process. The readings history at time t contains the most recent N sonar readings gathered until time t . It is defined as follows:

$$RH_t = \{z_{t-N+1}, \dots, z_{t-2}, z_{t-1}, z_t\} \quad (2)$$

The value of N has to be decided so that RH_t can store two consecutive full 360° scans. In our particular configuration a full MSIS scan is composed of 200 beams. Thus, N is set to 400.

Let \bar{x}_t denote the robot motion from time step $t-1$ to time step t . This robot motion is modeled as a RGV and is provided by the dead reckoning EKF. Similarly to the readings history, let the *transformations history* be defined as a history of the most recent N robot motions. That is,

$$TH_t = \{\bar{x}_{t-N+1}, \dots, \bar{x}_{t-2}, \bar{x}_{t-1}, \bar{x}_t\} \quad (3)$$

As the AUV is moving while acquiring the scan, each reading in RH_t may have been obtained at a different robot pose. The goal of the scan building process is to represent each reading in one scan with respect to a common coordinate frame.

Let us denote by $z_{i,j}$ the measurement $z_i \in RH_t$ represented with respect to the robot pose at time j , where $t-N+1 \leq i \leq t$ and $t-N+1 \leq j \leq t$, being t the current time step. $z_{i,j}$ can be computed as follows:

$$z_{i,j} = \begin{cases} z_i & i = j \\ \bar{x}_{j+1} \oplus \bar{x}_{j+2} \oplus \dots \oplus \bar{x}_i \oplus z_i & j < i \\ (\ominus \bar{x}_j) \oplus (\ominus \bar{x}_{j-1}) \oplus \dots \oplus (\ominus \bar{x}_{i+1}) \oplus z_i & i < j \end{cases} \quad (4)$$

where the operators \oplus and \ominus denote the compounding and inversion operations commonly used in the context stochastic mapping.

The robot motions involved in the Equation 4 are those in TH_t . Hence, by means of this equation, each reading in RH_t can be represented with respect to any coordinate frame referenced in TH_t while taking into account the robot motion. Next, it has to be decided which coordinate frame choose to build a scan. The chosen coordinate frame corresponds to the central position of the trajectory followed by the robot when collecting the readings involved in the scan.

The central position has been chosen for two main reasons. On the one hand, because of the similarity to the scans generated by a laser range finder. On the other hand, in order to reduce the maximum uncertainty of each reading with respect to the reference frame. Thus, every time the MSIS performs a 360° scan, S_{cur} is built as follows:

$$S_{cur} = \{z_{i,t_c}, \forall i, t - \frac{N}{2} < i \leq t\} \quad (5)$$

where t_c corresponds to the time step at which the robot was at the central position of the trajectory followed while the MSIS acquired the scan.

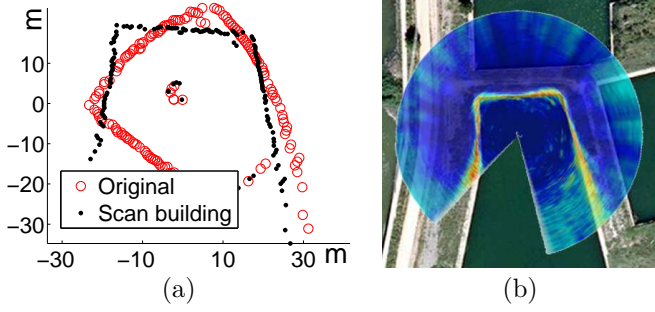


Fig. 4. (a) Range data before and after the scan building. (b) Acoustic image of one MSIS scan after the scan building.

In order to build the reference scan, the measurements that took part in the construction of S_{cur} in the previous scan matching execution are used. Therefore, the reference scan has the following form:

$$S_{ref} = \{z_{i,t_{c2}}, \forall i, t - N < i \leq t - \frac{N}{2}\} \quad (6)$$

where t_{c2} corresponds to the time step in which the robot was at the central position of the trajectory followed while the MSIS acquired the scan data. Figure 3-b graphically depicts the location of the coordinate frames and time steps used during the scan building process.

Figure 4-a illustrates the result of the scan building by the raw range data before and after the scan building. Additionally, 4-b shows the acoustic image corresponding to the corrected scan overlaid to a satellite view to show the effects of the correction.

It is important to emphasize that, due to the pose correction, which is described later in this paper, the robot motions stored in the transformations history may change. In consequence, S_{ref} has to be built at each scan matching execution by means of Equation 6. In other words, S_{cur} is not directly used in the next scan matching execution as S_{ref} because of possible changes in the transformations history between scan matching executions.

When the scan building has built S_{ref} and S_{cur} , the scan matching process is ready to be launched.

5. THE SONAR PROBABILISTIC ITERATIVE CORRESPONDENCE (SPIC)

The sonar scan matching process is in charge of finding the displacement and rotation x_B^A between the coordinate frames A and B of the two scans, S_{ref} and S_{cur} , built by the scan building. The sonar scan matching approach adopted in this paper is the spIC, which follows the same algorithmic structure that ICP. The main difference between the ICP and the spIC is that the former uses Euclidean distance whereas our proposal is based on the Mahalanobis distance to take into account the statistical information stored in the scans.

At the extent of the authors' knowledge, there is only one study prior to the spIC based on the use of such distance to perform scan matching. It is the pIC, proposed by Montesano et al. (2005) and adapted to underwater sonar by Hernández et al. (2009). However, the pIC approximates each set of correspondences by a normal distribution. This

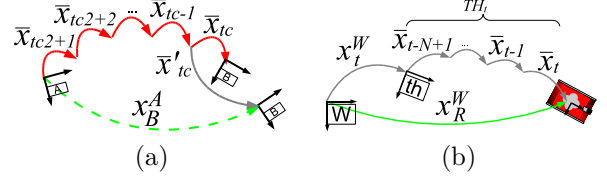


Fig. 5. (a) The pose correction process. (b) The pose extraction process. The term x_R^W denotes the robot pose.

approximation, as discussed by Burguera et al. (2008), is problematic when used in the context of terrestrial ultrasonic range finders. That is why this paper does not perform such approximation by adopting the spIC. The experimental results will show the benefits of this point of view. The description of this algorithm is out of the scope of this paper. A detailed description is available in the paper by Burguera et al. (2008).

6. POSE CORRECTION AND POSE EXTRACTION

The scan matching provides the estimate x_B^A of the displacement and rotation between the two scan coordinate frames, A and B . However, the scans have not been obtained at these frames. Instead, the scan readings have been obtained throughout a robot trajectory and the use of A and B is only a convenient way to represent the MSIS data. The goal of the *pose correction* is to correct the aforementioned robot trajectory so that it fits to the scan matching estimate.

A possible way to do this is to correct each motion estimate in the transformations history according to its uncertainty. This solution is the so called *trajectory correction* and is described by Burguera et al. (2008). The pose correction discussed in this paper is a simplified version of the trajectory correction that runs much faster at the cost of producing slightly less smooth trajectories. Instead of distributing the error correction through all the mentioned transformations history items, the pose correction performs one single change in the transformations history. Figure 5-a illustrates this idea.

From this Figure, it is easy to see that the mean of \bar{x}_{tc} should be corrected to the mean of \bar{x}'_{tc} as follows:

$$\bar{x}'_{tc} = \ominus(\bar{x}_{tc2+1} \oplus \dots \oplus \bar{x}_{tc-1}) \oplus x_B^A \quad (7)$$

The covariance of the corrected transformations history item, P'_{tc} , is also needed. Unfortunately, the covariance of \bar{x}'_{tc} is not a good approximation because it accumulates the uncertainties of $\ominus(\bar{x}_{tc2+1} \oplus \dots \oplus \bar{x}_{tc-1})$ and x_B^A . To ease notation, let $x_{th} = N(\hat{x}_{th}, P_{th})$ be defined as $\bar{x}_{tc2+1} \oplus \dots \oplus \bar{x}_{tc-1}$. By performing some algebraic manipulation on the \oplus and \ominus definitions, the covariance can be computed as follows:

$$P'_{tc} = J_{2\oplus}^{-1}(P_B^A - J_{1\oplus}P_{th}J_{1\oplus}^T)(J_{2\oplus}^T)^{-1} \quad (8)$$

where the terms $J_{1\oplus}$ and $J_{2\oplus}$ are the Jacobians matrices of the composition, as defined in Tardós et al. (2002).

This equation can only be used if the eigenvalues of P_B^A are smaller than those of P_{th} . Otherwise, the resulting P'_{tc} will not be positive definite and, thus, not actually be a covariance matrix. As a matter of fact, in these cases the

covariance P'_{tc} does not even exist. A possible way to deal with these situations is to leave the covariance unchanged in the transformations history. The experimental results suggest that the error introduced by this simplification is negligible.

Contrarily to the pose correction, which is only executed after the scan matching, the *pose extraction* operates continuously and provides robot pose estimates from the transformations history. This is accomplished by maintaining an estimate x_t^W of the first item in the transformations history with respect to a fixed coordinate frame. This estimate is updated every time an item from the transformations history is discarded. Then, x_t^W is compounded with all the remaining items in the transformations history. The current robot pose, x_R^W , is obtained in this way, as illustrated in Figure 5-b.

7. EXPERIMENTAL RESULTS

The experimental data used to validate the uspIC was obtained by Ribas et al. (2008) in an abandoned marina situated near St. Pere Pescador in the Costa Brava (Spain). The Ictineu AUV was teleoperated along a 600m trajectory at an average speed of 0.2m/s. The trajectory includes a small loop as well as a 200m long straight path. The gathered data included measurements from the DVL, the MRU and the MSIS. Additionally, a buoy with a GPS was attached to the robot in order to obtain the ground truth.

In order to evaluate the proposal in this paper, the uspIC is compared to two approaches to scan matching using a MSIS. On the one hand, the MSISpIC by Hernández et al. (2009). This approach is based on the so called *scan grabbing*, which is in charge of segmenting the MSIS beams and collecting them to build scans, and the pIC algorithm to perform the matching. On the other hand, the *Underwater Sonar ICP* (usICP). This approach consists on performing the same beam segmentation, scan building, pose correction and pose extraction processes described in this paper but using the ICP to perform the matching.

7.1 Quantitative Evaluation

The trajectories estimated by dead reckoning, usICP, MSISpIC and uspIC have been compared to the ground truth provided by the GPS. The comparison consists in measuring, at each time step, the distance from the GPS ground truth to the estimated robot pose according to each of the mentioned methods. Figure 6-a compares usICP and uspIC. The uspIC error is below the usICP one during 69.53% of the time. Moreover, among the compared methods, the uspIC is the only one that has provided better results than dead reckoning during the 100% of the time. Figure 6-b compares the uspIC and the MSISpIC and shows that the uspIC provides better pose estimates than MSISpIC during the 73.62% of the time. Moreover, we have observed that usICP provides better estimates than MSISpIC a 65.28% of the time. According to this, the scan matching approach that provides better results during the most part of the time is the uspIC, followed by the usICP and the MSISpIC, in this order. Table 1 summarizes these results by showing the mean error, the maximum error and the standard deviation of the error.

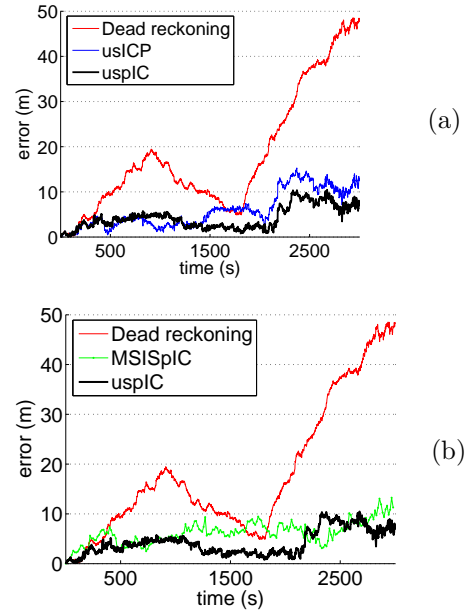


Fig. 6. Quantitative evaluation, comparing dead reckoning with (a) uspIC and usICP, and (b) uspIC and MSISpIC.

Method/Error	Mean	Maximum	Std. Dev.
Dead Reckoning	18.32m	49.03m	13.64
MSISpIC	6.19m	13.25m	2.26
usICP	6m	15.29m	4
uspIC	4.21m	10.47m	2.5

Table 1. Maximum, average and standard deviation of the error for the tested methods.

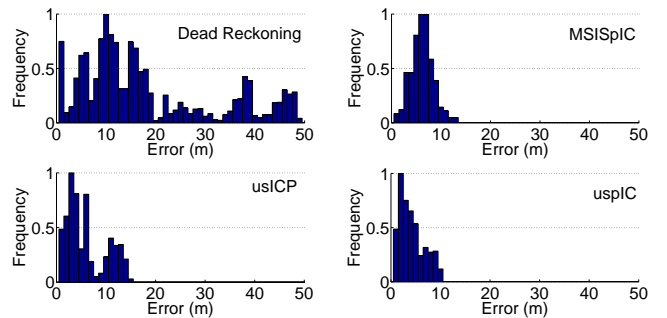


Fig. 7. Histogram of the error for dead reckoning, MSISpIC, usICP and uspIC. The error frequency has been normalized for clarity purposes.

Figure 7 shows the histograms of the localization error. The histograms clearly reflect the aforementioned maximum error. Moreover, the histogram provides information about how this error is distributed. For example, it is clear that the dead reckoning error spreads over a large region but the most part of it is concentrated between 0m and 20m of error. It is remarkable that the most part of the usICP error is around the 3m, which is significantly below the 6m of the MSISpIC. However, the usICP errors spread over a larger area than MSISpIC, and that is why both approaches have a similar average error. Finally, it is also remarkable that the uspIC is not only the method with the lowest maximum error, but also that the most part of the error is concentrated around 2m.

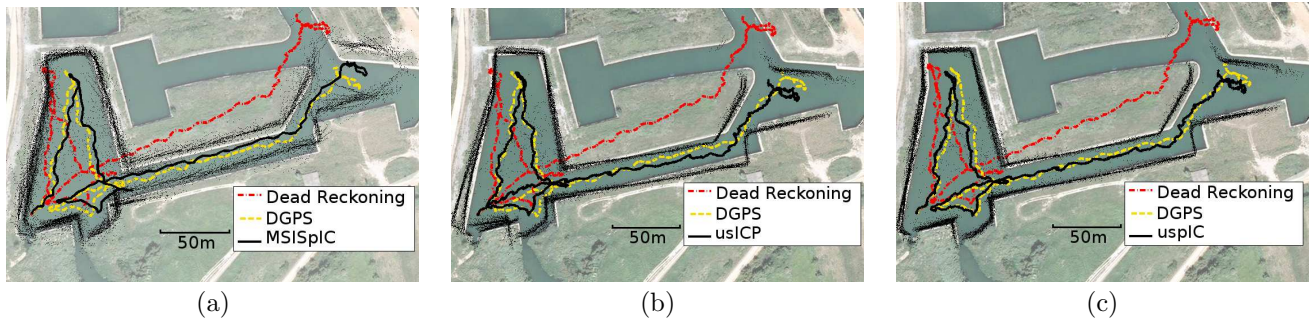


Fig. 8. Trajectories corresponding to GPS, dead reckoning and (a) MSISpIC, (b) usICP and (c) uspIC.

7.2 Qualitative Evaluation

Figure 8 shows the trajectories obtained by MSISpIC, usICP and uspIC and visually compares them to the ones provided by dead reckoning and the GPS ground truth. Moreover, the data is superimposed to a satellite view of the area to provide a clear idea of the quality of the obtained trajectories. The first thing to be noticed is that the three methods produce a trajectory close to the ground truth, especially when it is compared to the dead reckoning data. Besides, there are some differences that deserve special attention.

Firstly, the MSISpIC (Figure 8-a) has not been able to solve the double wall effect on the left side of the image, although the effect has been significantly reduced with respect to dead reckoning. This effect appears when the AUV returns to a previously visited area with a significant pose error. Also, the data corresponding to the entrance to the canal is misaligned, similarly to dead reckoning, where two entrances to the canal seem to exist.

Secondly, the usICP (Figure 8-b) has, similarly to dead reckoning and MSISpIC, the problem of perceiving a double wall on the left side of the image. However, contrarily to MSISpIC, the usICP has been able to align the data corresponding to the canal entrance. Moreover, it can be observed that the trajectory provided by usICP is slightly shorter than the one provided by MSISpIC. This difference is due to the canal shape. As the canal is almost straight, it is very difficult for a scan matching algorithm to determine the robot motion along the corridor direction.

Finally, the uspIC (Figure 8-c) is the algorithm that clearly exhibits better results. First, the double wall effect does not appear. Moreover, the canal entrance data is perfectly aligned. Also, at the end of the experiment, the uspIC is the approach whose pose estimate is the closest to the ground truth. It can also be observed that the uspIC data fits the satellite image better than the other methods, especially on the water tank on the left.

8. CONCLUSION

This paper presents a novel approach to localize an underwater mobile robot. The localization process, which also relies on some proprioceptive sensors to perform dead reckoning, is focused on the use of a MSISpIC. The approach presented in this paper is the so called uspIC, which deals with the MSISpIC problems.

The experimental results compare the uspIC to other previously existing methods: the ICP and the MSISpIC, which is an underwater scan matching method that utilizes the pIC concepts. The obtained results show an important improvement in the pose estimate with respect to the other tested methods. Some graphical representations of the obtained trajectories have also been provided for the reader to visually compare them.

ACKNOWLEDGEMENTS

The authors are grateful to David Ribas, Pere Ridao and Emili Hernández from Universitat de Girona for the data sets and for their advice regarding the MSISpIC algorithm.

REFERENCES

- Besl, P. and McKay, N. (1992). A method for registration of 3-d shapes. *IEEE Transactions on Pattern Analysis and Machine Intelligence*, 14(2), 239–256.
- Burguera, A., González, Y., and Oliver, G. (2008). A probabilistic framework for sonar scan matching localization. *Advanced Robotics*, 22(11), 1223–1241.
- Censi, A. (2008). An ICP variant using a point-to-line metric. In *Proceedings of the IEEE International Conference on Robotics and Automation (ICRA)*. Pasadena, CA.
- Hernández, E., Ridao, P., Ribas, D., and Batlle, J. (2009). MSISpIC: A probabilistic scan matching algorithm using a mechanical scanned imaging sonar. *Journal of Physical Agents*, 3(1), 3–11.
- Lu, F. and Milios, E. (1997). Robot pose estimation in unknown environments by matching 2D range scans. *Journal of Intelligent and Robotic Systems*, 18(3), 249–275.
- Montesano, L., Minguez, J., and Montano, L. (2005). Probabilistic scan matching for motion estimation in unstructured environments. In *Proceedings of the Conference on Intelligent Robots and Systems (IROS)*, 1445–1450.
- Ribas, D., Ridao, P., Tardós, J., and Neira, J. (2008). Underwater SLAM in man made structured environments. *Journal of Field Robotics*, 11-12(25), 898–921.
- Tardós, J.D., Neira, J., Newman, P.M., and Leonard, J.J. (2002). Robust mapping and localization in indoor environments using sonar data. *International Journal of Robotics Research*, 21(4), 311–330.